Volume 51 | Number 34 | 30 April 2015 | Pages 7263–7406

ChemComm

Chemical Communications

www.rsc.org/chemcomm

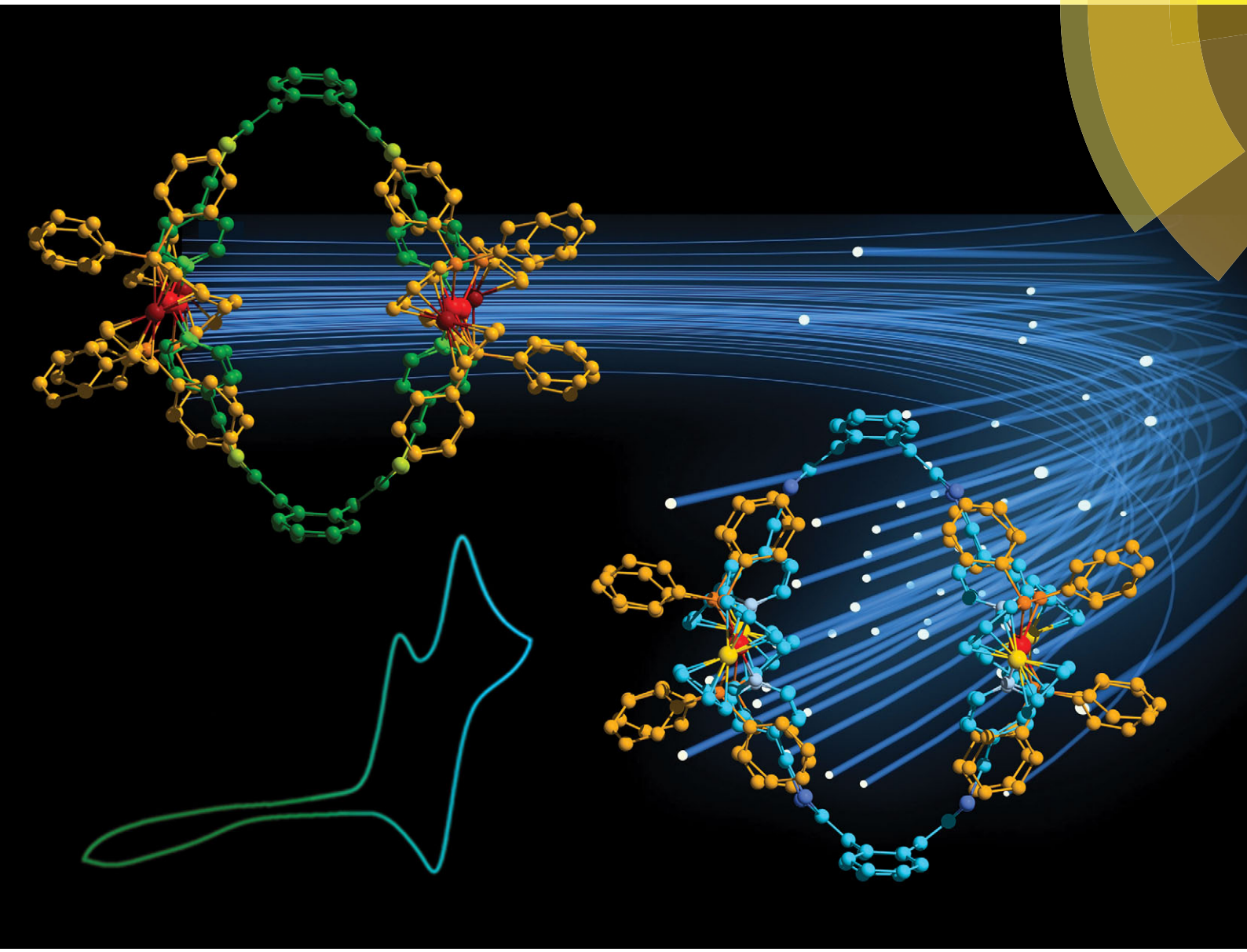

ISSN 1359-7345

ROYAL SOCIETY OF CHEMISTRY

FEATURE ARTICLE

S. Goeb, M. Sallé *et al.*

Metal-driven self-assembly: the case of redox-active discrete architectures

ChemComm

FEATURE ARTICLE

View Article Online
View Journal | View Issue

Cite this: *Chem. Commun.*, 2015, **51**, 7275

Metal-driven self-assembly: the case of redox-active discrete architectures

V. Croué, S. Goeb* and M. Sallé*

Received 21st January 2015,
Accepted 17th March 2015

DOI: 10.1039/c5cc00597c

www.rsc.org/chemcomm

The metal-driven self-assembly strategy is well-established for the construction of discrete architectures featuring a cavity. The resulting molecular rings and cages are potentially useful as hosts for complementary guests. Recent years have seen growing interest in the introduction of given functionalities, including redox properties which, among others, allow modulating the ionic charge of the cavity. Depending on which subunit is electroactive, various situations can be encountered, with a global redox activity which is ligand- and/or metal-centered and which involves or not electronic interactions between the constituting units. In this feature article, we propose to survey those different situations by exploring some recent examples of the growing family of redox-active self-assembled rings and cages.

Introduction

The self-assembly methodology, more particularly when assisted by metals, constitutes a very efficient synthetic approach[1] to obtain more and more sophisticated macrocyclic structures, otherwise very challenging to prepare through

Université d'Angers, CNRS UMR 6200, Laboratoire MOLTECH-Anjou, 2 bd Lavoisier, 49045 ANGERS cedex, France. E-mail: sebastien.goeb@univ-angers.fr, marc.salle@univ-angers.fr; Fax: +33 241 735 405; Tel: +33 241 735 439

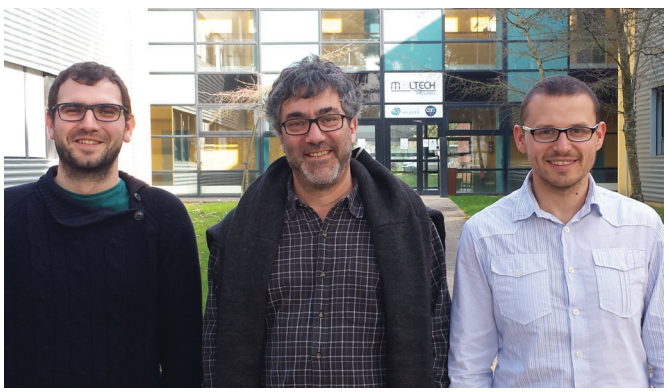

From left to right: V. Croué, M. Sallé and S. Goeb

Vincent Croué (left) was born in Angers (France) in 1989. He obtained his Master's Degree from the University of Angers in Molecular Engineering and Nanotechnologies in 2012 working on TTF derivatives for metal-directed self-assembly. Since then, he has been a PhD Student in Organic Chemistry in Prof. Marc Sallé's team. His research interests mainly concern discrete redox active self-assembled cages incorporating extended-TTF units.
Dr Sébastien Goeb (right) was born in Schiltigheim (France) in 1979. He studied chemistry at the University of Strasbourg and obtained his PhD degree in Organic Chemistry in 2006 under the supervision of Drs Raymond Ziessel and Antoinette De Nicola. He then carried out two successive one year postdoctoral stays respectively with Prof. Felix N. Castellano at the University of Bowling Green (USA) and with Dr Jean-Luc Parrain at the Institut des Sciences Moléculaires de Marseille (France). He became Chargé de Recherche CNRS in the laboratory MOLTECH-Anjou in 2008. His research interests focus on the organic chemistry of photo- and/or redox-active supramolecular discrete architectures.
Prof. Marc Sallé (middle) was born in Toulon (France) in 1963. He studied chemistry at the Ecole Nationale Supérieure de Chimie de Rennes (ENSCR) and at the University of Paris VI. He received his PhD degree in Organic Chemistry from the University of Angers in 1991 under the supervision of Professor Alain Gorgues. For this work he was awarded the Dina Surdin prize of year 1992. After a postdoctoral stay with Prof. Martin R. Bryce at the University of Durham (UK), he became Maître de Conférences at the University of Angers, where he was promoted to a professor in 1998. He has been a junior member of the Institut Universitaire de France (IUF). His research interests concern the organic chemistry of molecular materials and supramolecular chemistry associated with electro(photo)-active molecular systems. Prof. Marc Sallé is currently the director of the Laboratory MOLTECH-Anjou (Angers, France).

classical step-by-step covalent synthesis. In order to target applications,[2] the resulting discrete structures, be they polygons or cages, may integrate various functionalities. In particular, there is great interest in responsive coordination-driven self-assembled architectures currently, which can be constructed through applying external stimuli, as for example irradiation with light.[3] On these grounds, there is growing interest in assemblies responsive to a redox-stimulus and the number of electro-active metalla-rings/cages has been increasing drastically in the very recent years. The use of redox-active precursors in the self-assembly process can in principle produce discrete metalla-supramolecular assemblies which are redox-active. Various situations can be encountered, *e.g.* electroactivity which is brought about either by the organic ligand part (naked or appended with a redox-active unit), by the metal or by a co-ligand. Moreover, through-space or through-bond interactions between the different components can potentially occur. An immediate consequence with such a variety of situations lies on the possibility to switch, providing a suitable design, the ionic charge surrounding the cavity, by a simple tuning of the applied redox potential. It is worth noting that in addition to being redox-active, such systems intrinsically present a cavity which can therefore be used to bind a complementary guest.[4] This combination of properties is of particular importance for applications such as sensing or controlling encapsulation/delivery processes of various guests. Finally, the supramolecular assembly approach may constitute a promising future strategy to address the design of organic materials (*e.g.* organic photovoltaics and molecular electronic devices). Indeed, mastering the geometry of multicomponent redox-active systems offers a unique opportunity to fine-tune electronic interactions within the material,[5] which includes control over through-space electron hopping or delocalization and which is of prime importance for optimizing electron transport in organic materials.

Altogether, the diversity of the redox-active structures which can be attained by the metal-driven self-assembly methodology opens fascinating perspectives for various research topics, ranging from drug delivery, guest sensing, catalysis or even molecular electronics. We propose in this feature article to cover the most recent advances in this field.

Metalla-rings/cages involving electron-poor ligands

2,4,6-Tris(4-pyridyl)-1,3,5-triazine-based cages

A prototypal self-assembled host system corresponds to the M_6L_4 cage **1** (Fig. 1a) extensively developed by M. Fujita and colleagues, which integrates triazine panels (2,4,6-tris(4-pyridyl)-1,3,5-triazine) and square-planar Pd(II) or Pt(II) as metal corners.[1u,6] Because of the three coordinated pyridine moieties, the tridentate triazine core is highly electron-poor. The redox properties of this assembly have been studied in order to address the photoinduced host–guest electron-transfer occurring between panels and alkanes encapsulated within the cavity.[7] In particular, this cage is able to form a clathrate complex

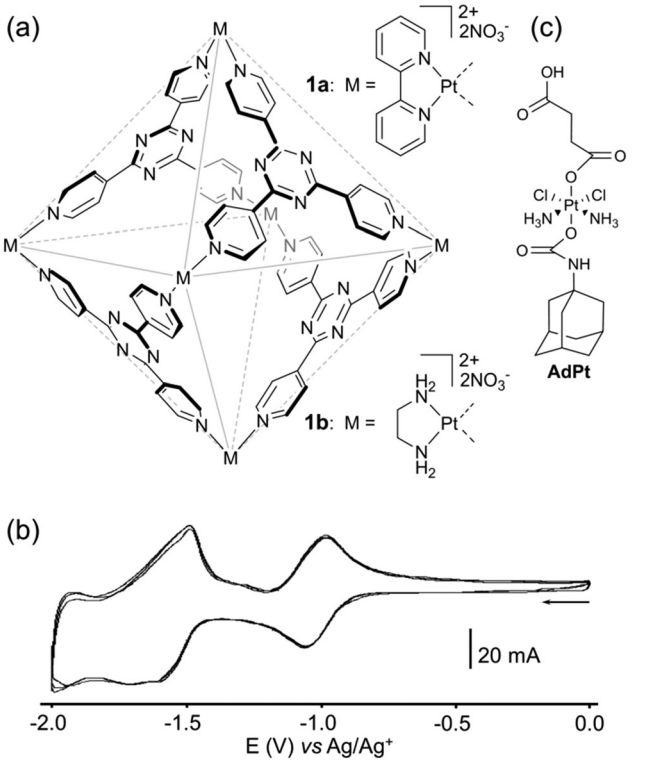

Fig. 1 (a) Structure of self-assembled molecular hosts **1a–b**; (b) cyclic voltammogram of **1b**: C = 0.5 mM in CH_3CN (Bu_4NPF_6 (50 mM)), scan rate 100 mV s^{-1}, (c) structure of **AdPt**.

with four adamantane molecules (**1a**⊃(adamentane)$_4$). Upon irradiation, the colourless solution of **1a**⊃(adamentane)$_4$ turns blue, indicating the generation of radical species. The photolysis of the complex produces two oxidized derivatives (1-adamantyl peroxide and 1-adamentanol) in a total yield of ~24% which indicates that only one among the four adamentanes has reacted.[8] The proposed reaction mechanism involves the generation of the host anion-radical and guest cation-radical *via* a guest-to-host photoinduced electron transfer (PET), with only one triazine panel involved. The cyclic voltammetry of cage **1b** was investigated and exhibits two redox systems (Fig. 1b). A reversible redox wave corresponding to a one-electron process, as confirmed by coulometric experiments and as supported by DFT calculations, is observed at $E = -1.02$ V *vs.* Ag/Ag^+, followed by pseudo-reversible redox waves from $E = -1.40$ to -2.00 V, assigned to three electrons in total. It is worth noting that in the case of cages **1a,b**, the four triazine panels are not simultaneously reduced which is due to the electronic communication occurring between the side walls of the cage through the Pt ion centers.

Such a propensity of cage **1b** to bind adamantane was very recently explored by J. T. Lippard and coworkers for drug delivery purposes.[9] The authors developed a well-defined Pt drug delivery system based on the encapsulation of four adamantyl groups inside the cavity, each of them being appended with a Pt(IV) prodrug unit (**AdPt**). The cyclic voltammetry of assembly **1b**·**AdPt**$_4$ in water shows cathodic signals assigned to the triazine core (**1b**), as well as a less negative one corresponding to the irreversible reduction of Pt(IV). This scheme

is confirmed by a chemical reduction of **1b**·**AdPt**$_4$ with ascorbic acid, which gives rise to a cisplatin release, beside 1-adamantylamine and succinic acid, providing therefore a proof of concept for a controlled delivery of cisplatin through reduction.

Finally, one can remind that tris(pyridyl)-triazine cages **1a,b** present a good ability to encapsulate a wide variety of organic guests.[1u] This property was explored in the peculiar case of redox-active guests such as organic radicals of the nitronyl nitroxide type[10] or ferrocene derivatives,[11] whose redox properties are significantly modified upon encapsulation.

Rhenium-based rings and cages

The redox properties of the same tridentate triazine panel, in association with indigo anions and Re(I), were recently studied by C.-Y. Lin, K.-L. Lu and coworkers in the case of the neutral self-assembled triangular metalloprism **2** (Fig. 2a), which exhibits strong NIR absorption.[12] The presence of electron-accepting indigo and triazine units in the same structure makes this metalloprism highly electron-poor and easy to reduce. Actually, **2** can be electrochemically switched to several polyanionic states through stepwise reduction processes involving up to eight electrons, giving rise to an efficient control over the corresponding optical properties. Four reversible reduction waves are observed from cyclic voltammetry experiments (Fig. 2b). Remarkably, this study coupled with EPR analysis and DFT calculations indicates that the stepwise reduction sequence is essentially ligand-centered. The first redox system at E = −0.29 V *vs.* Ag/AgNO$_3$ is ascribed to the simultaneous one-electron reduction of three indigo ligands giving rise to $\mathbf{2}^{3\bullet-}$, the latter species corresponding to a metal-bound indigo radical anion exhibiting a small dπ-Re-indigo orbital mixing. The second and third reductions (E = −0.73 and −0.98 V) are tentatively assigned to one electron reductions of each triazine ligand, which is supported by EPR experiments. The splitting of these two reduction waves may be ascribed to a stabilization of a mixed-valence state between the facing tris(pyridyl)triazine units,[13] a behavior which is not observed between the indigo pillars which are distant from each other. The fourth reduction process (E = −1.23 V) corresponds to the second one-step three-electron-reduction process at the indigo-pillared ligands. Interestingly, the metalloprism **2** can be also reversibly oxidized through a three-electron process, corresponding to the oxidation of each indigo dianion. It appears from these data that the structure **2** behaves as an electron reservoir endowed with programmed and well-defined redox-properties.

Another rhenium-based family of redox-active polygons corresponds to rectangles **3a–f** depicted by J. T. Hupp and coworkers (Fig. 3a).[14] The latter incorporate four Re(I) corners which are organized into two pairs by doubly chelating planar 2,2′-bisbenzimidazolate ligands and which are bridged by rigid or semirigid ditopic symmetrical (LL) ligands. These systems were designed to study the balance between intramolecular through-space electronic communication (between facing LL ligands) *vs.* coordination-bond-mediated interactions. Spectroelectrochemical studies conducted at the −1 charge state of the rectangles (*i.e.* mixed-valence state with respect to the ligands), demonstrated that those systems are dominated by electronic interactions of the former type. A cyclic voltammetry study of rectangles **3a–f** was carried out and shows reversible reduction waves that are assigned to stepwise one-electron reductions of the symmetrical LL ligands within the rectangle (for a representative example, see the case of compound **3d**, Fig. 3b). No oxidative wave is observed and the reduction potentials appear substantially shifted to less negative potentials in comparison with free ligands, which is due to the electrostatic stabilization

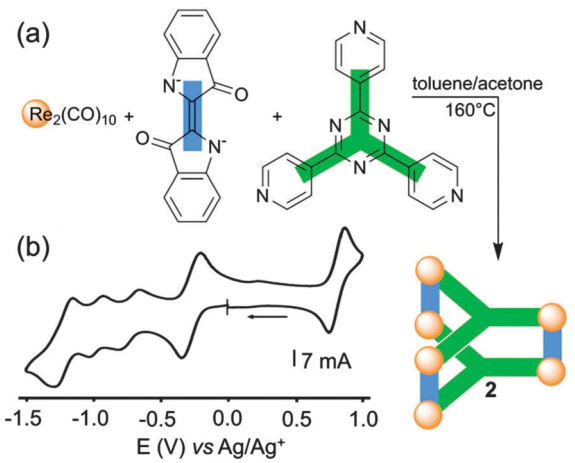

Fig. 2 (a) Orthogonal-bonding approach for the preparation of metalloprism **2**; (b) cyclic voltammogram of **2**: C = 1 mM in THF (Bu_4NPF_6 (0.1 M)), scan rate 100 mV s^{-1}.

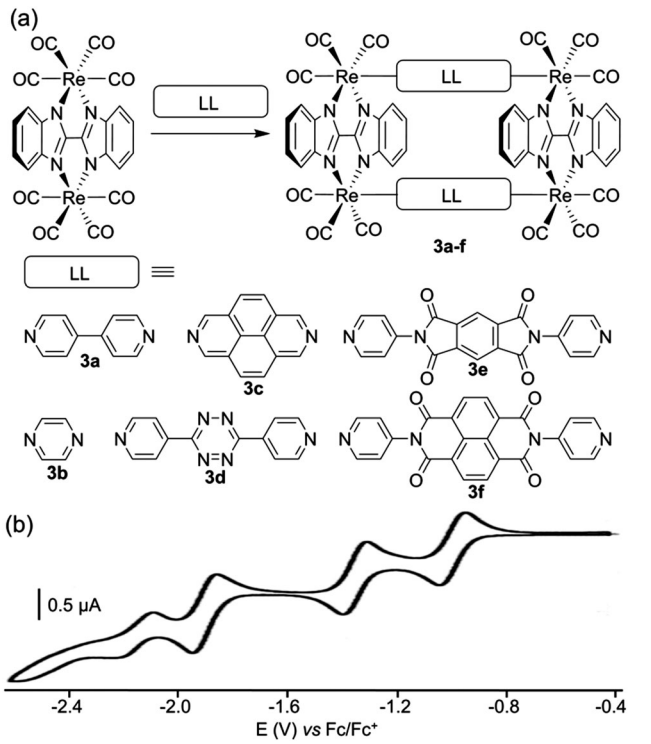

Fig. 3 (a) Rhenium-based molecular rectangles **3a–f**; (b) cyclic voltammogram of **3d** in THF (Bu_4NPF_6 (0.1 M)).

promoted by the rhenium cations over the negative reduced forms of the ligands.

Perylene bisimide-based rings and cages

F. Würthner and colleagues have developed a series of self-assembled discrete architectures based on the photo- and electroactive perylene bisimide (PBI) unit. A prototypal example corresponds to metalla-square **4**,[15] constructed from a tetraaryl-substituted *N*,*N*′-4-pyridyl-substituted PBI ligand and a square planar Pt(II) complex (Fig. 4a). The UV/Vis and fluorescent properties of square **4** are not significantly changed compared to those of the PBI-ligand precursor, which is explained by the lack of electronic communication through the imide substituent. The cyclic voltammetry of square **4** (Fig. 4b) reveals two successive reversible reduction waves at $E = -1.01$ and -1.14 V *vs.* Fc/Fc^+, which are slightly shifted compared to the free ligand PBI-ligand precursor ($E = -1.08$ and -1.23 V respectively). They correspond to the successive radical anion and dianion formation for each perylene unit, which behave independently contrary to the above-presented triazine-based cages, which is also confirmed by the spectroelectrochemical study conducted on **4** that exhibits redox processes which are exclusively ligand-centered. Finally, a reversible oxidation process is observed for the metalla-square **4** at $E = +0.93$ V *vs.* Fc/Fc^+. Therefore, this electrochemical study demonstrate that the ionic state of square **4** can be in principle reversibly tuned from 0 to +12, in three steps of four electrons. Ultimately, this CV study also confirms the electrochemical inertness of the Pt(II) phosphane corner in the $E = -1.30$ V to +0.90 V range (*vs.* Fc/Fc^+), this complex being one of the most commonly used for the construction of discrete self-assembled metalla-rings and cages *via* the coordination-driven approach. As demonstrated by the same group, the PBI panels can also be functionalized with pendant redox-active units such as in metalla-square **5** (Fig. 4a) decorated with 16 redox ferrocene moieties.[16] Consequently, in addition to the typical reduction of each PBI unit to the radical anion and dianion states ($E = -0.98$ and -1.13 V *vs.* Fc/Fc^+ respectively), compound **5** also exhibits oxidation of the ferrocenyl groups (Fig. 4c). Noteworthy, contrary to the reduction of the four PBI panels which occurs simultaneously in **5**, the peripheral ferrocene units give rise to a splitting of the ferrocene/ferricinium redox wave, a consequence of through-space interactions occurring between ferrocene units in such a confined space.

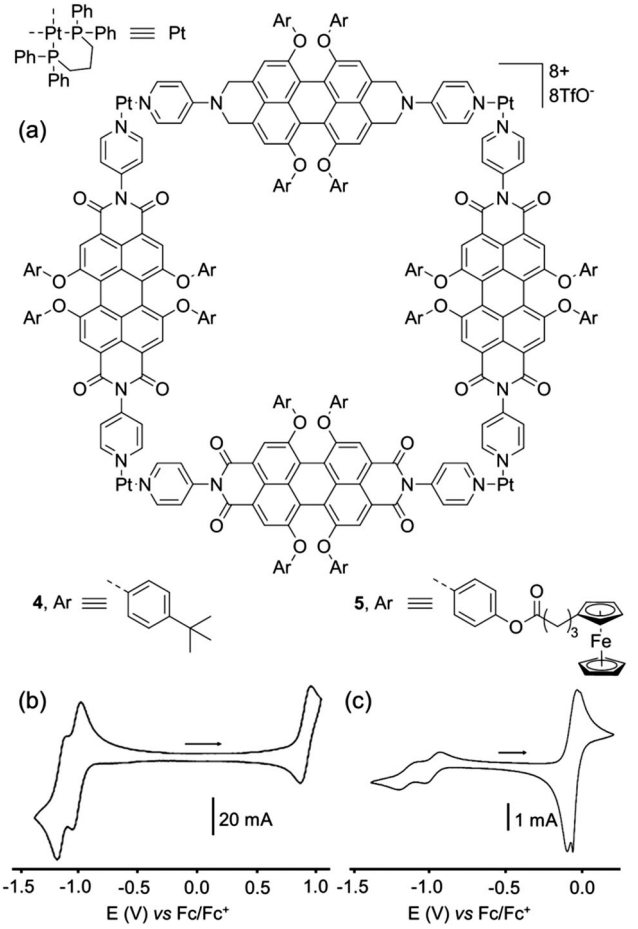

Fig. 4 (a) Metallosupramolecular squares **4** and **5**. Cyclic voltammogram of **4** (b) and **5** (c) in CH_2Cl_2 (Bu_4NPF_6 (0.1 M)), scan rate 100 mV s^{-1}.

Though presenting remarkable photophysical and electrochemical characteristics as well as defined cavities, no guest encapsulation from the above-described PBI-based metalla-macrocycles was mentioned by the authors. It is only very recently that the same group designed a robust PBI-based metalla-assembly presenting host–guest properties.[17] The very large M_4L_6 tetrahedron **6** (Fig. 5a) is assembled from an octahedral Fe(II) ion and a PBI ligand bearing 2,2′-bipyridine units on the imide positions. The resulting $Fe_4(PBI)_6$ tetrahedron exhibits a particularly rich electrochemical activity manifested by multiple redox processes. As seen above, PBI derivatives are electron-accepting moieties that can be successively reduced into radical-anion and dianion species. This is observed in the CV of **6** which exhibits reversible redox waves at $E = -0.94$ and -1.11 V *vs.* Fc/Fc^+ respectively (Fig. 5b). Moreover, assembly **6** incorporates four electroactive $Fe(bpy)_3^{2+}$ centers which are known to undergo reversible electrochemical oxidation and reduction processes. The reductions of the bpy units on each metal center are not simultaneous and occur according to three successive one-electron reduction processes, giving rise to a total of five reversible reduction waves for assembly **6**. In addition, two oxidation waves are observed at $E = +0.73$ and +0.95 V *vs.* Fc/Fc^+, assigned to the successive Fe^{2+} and PBI oxidation. It is worth noting that tetrahedron **6** is redox-stable for an impressive broad range of charges (from -16 up to +18), which corresponds to a total of 34 electrons which can be switched, simply by controlling the electrochemical potential. The authors attribute this efficient charge balance to the highly porous character of the large tetrahedron **6**, which allows a suitable mobility of counterions during the redox switches. Another consequence of the large size of the cavity lies on the ability of **6** to encapsulate C_{60}. Moreover, the size complementarity is strengthened by the well-established electronic affinity between C_{60} and the PBI moiety. Actually, the authors have shown by ESI-TOF mass spectrometry that not only one, but two fullerene units can be encapsulated within

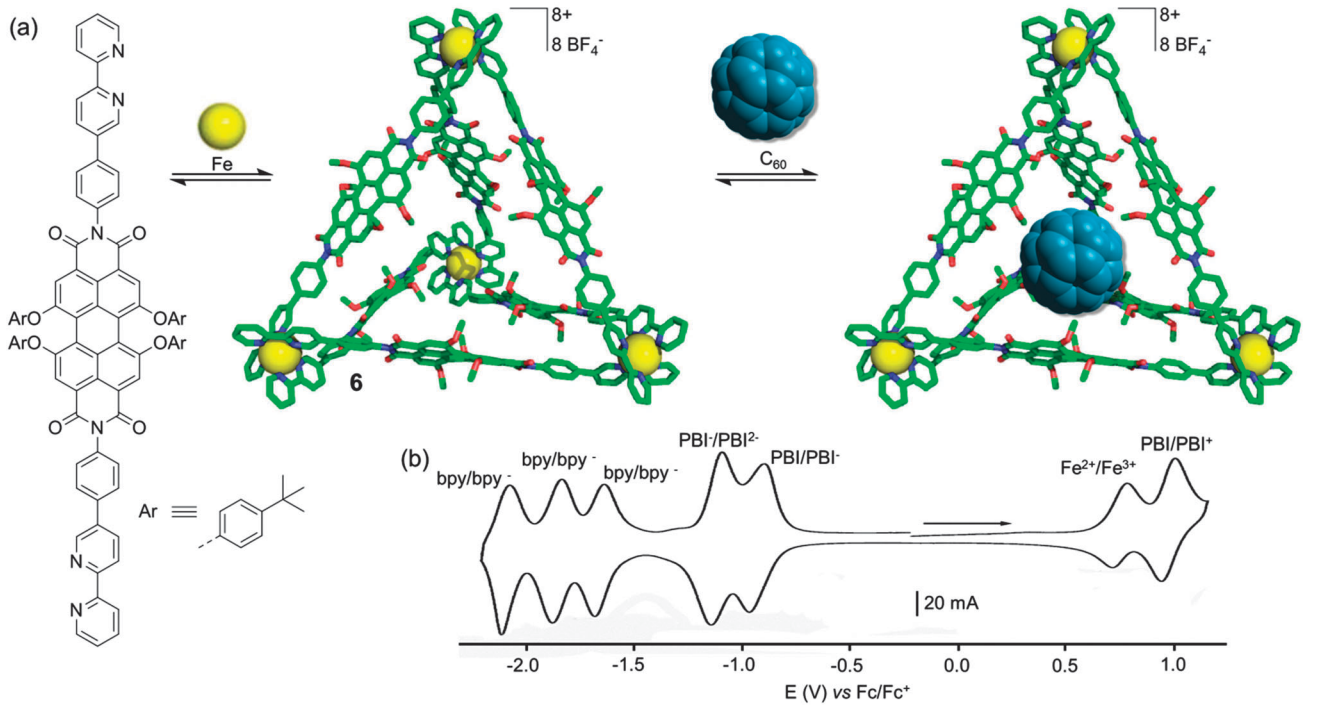

Fig. 5 (a) Self-assembly of metallosupramolecular tetrahedron **6** and C_{60} encapsulation; (b) cyclic voltammogram of **6**: C = 0.1 mM in CH_3CN (Bu_4NPF_6 (0.1 M)), scan rate 200 mV s^{-1}.

tetrahedron **6**, which is one of the largest cavity ever described for the M_4L_6 family.

Metalla-rings/cages involving electron-rich ligands

Rings and cages incorporating ferrocene subunit(s)

The design and the synthesis of molecular systems constituted from several redox-active units within the same assembly is attractive for various applications such as photochemical devices or information storage. In this context, in addition to the PBI-based assembly **5** described above, several electro-active self-assembled rings and cages decorated with multiple Fc units were reported, notably by the groups of P. J. Stang, H.-B. Yang and coworkers. Using the straightforward coordination-driven self-assembly strategy, the authors were able to build both hexagonal[18] and triangular[19] supramolecular metalla-cycles incorporating ferrocenyl moieties either inside[18a] or outside[18b,c,19] the cavity. The general synthetic methodology involves the rational combination of ferrocenyl skeletons presenting 120° (target = hexagons) or 60° (target = triangles) coordination sites, with complementary linear units. For example, the synthesis depicted below (Fig. 6a), involves a linear 4,4′-bipyridine ligand with bis-metallic complexes bearing one (target = **8**)[18b] or two (target = **7**)[19] pendant ferrocenyl group(s). For the preparation of hexagons, an alternative approach consists of the combination of two complementary 120° oriented electro-active building blocks (**9**).[18b] Electrochemical properties of the resulting multi-ferrocenyl complexes were studied by cyclic voltammetry. All hexagonal assemblies

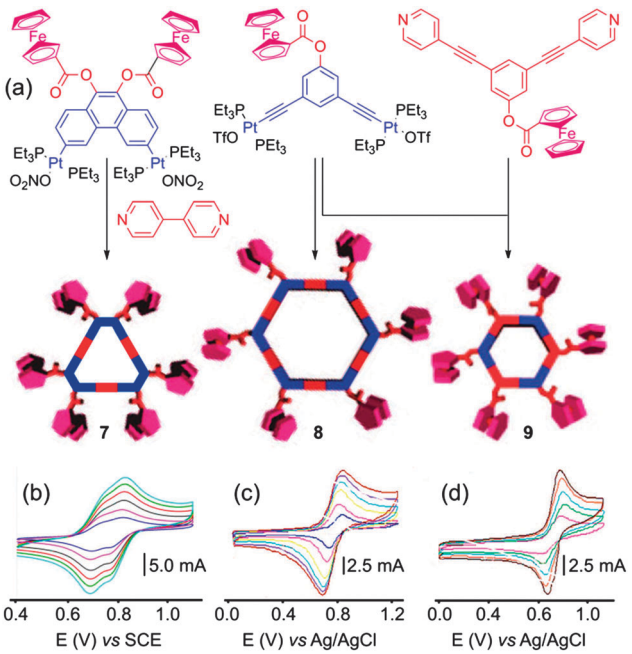

Fig. 6 (a) Synthesis of self-assemblies **7**, **8** and **9**; cyclic voltammogram of **7** (b), **8** (c), **9** (d): C = 0.20 mM in CH_2Cl_2 (Bu_4NPF_6 (0.15 M)), scan rate 25–250 mV s^{-1}.

exhibit a single reversible redox wave with several electrons transferred during the oxidation process indicating that all ferrocene units react independently (see example of assemblies **8** and **9**, Fig. 6c and d). Due to the large cavity size, this phenomenon

occurs even when the ferrocenyl units point towards the center of the cavity.[18a] Remarkably, the redox-active character of the pendant Fc probes provides a unique opportunity to address a quantitative approach which can be supported by electrochemical studies. In particular, the diffusion coefficient (*D*) of the metalla-cycles could be estimated from the Randles–Sevcik equation by measuring the peak intensity at different scan rates or by potential-step chronoamperometry. The determined *D* values suitably correlate with the corresponding hydrodynamic diameters of the self-assembled architectures, as expected from the inverse proportionality between *D* and the metalla-macrocycle size. Therefore, the Fc units offer here an original way to probe electrochemically the size of the edifice, which is in principle complementary to DOSY NMR experiments. Finally, unlike hexagonal assemblies **8** and **9**, it has to be noted that in the case of compound **7**,[19] the presence of two spatially close Fc units at vicinal positions of each phenanthrene moiety results in a splitting of the associated redox wave in the cyclic voltammogram (Fig. 6b). Such behaviour is assigned to a through-space electronic communication between the two proximal Fc units.

With the aim of producing supramolecules that combine multiple properties, the same authors recently depicted multifunctional systems associating both an electro-active unit (*i.e.* Fc) and a crown-ether binding site in a same self-assembled macrocycle (Scheme 1).[20] The single redox wave corresponding to the ferrocene unit in compound **10** remains reversible, and allows for the determination of the corresponding *D* values. Its binding properties with a dibenzyl ammonium salt were studied by ^{1}H NMR and cyclic voltammetry. No change in the half-wave potential was observed upon complexation of the dibenzyl ammonium guest, indicating the lack of interaction between pendant Fc and crown-ether subunits. Nevertheless, the voltammogram shape of complex **11** compared to free **10** indicates as expected a lower *D* value upon complexation. Finally, efforts towards the synthesis of electroactive dendritic metalla-assemblies have to be mentioned.[21] Based on a similar *exo*-functionalization approach as for the metalla-cycles depicted above, the same groups prepared a series of metallodendrimers of controlled size and shape, bearing both Fc and dendron functional groups. For instance, the reaction between

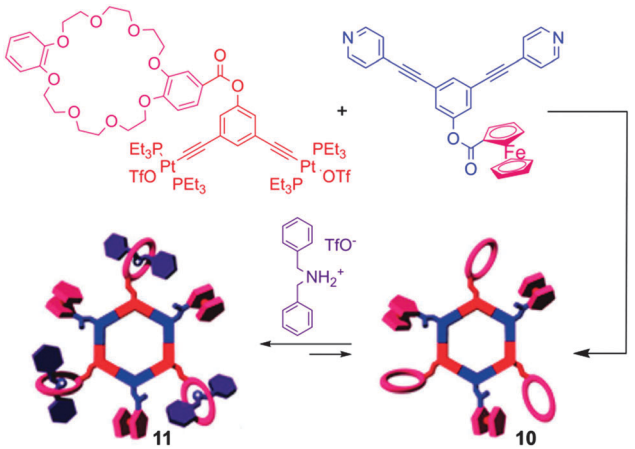

Scheme 1 Synthesis of self-assembly **10** and tris[2]pseudorotaxane **11**.

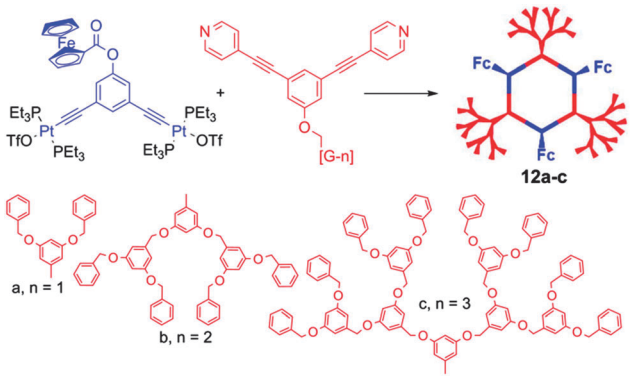

Scheme 2 Synthesis of dendritic multiferrocenyl hexagons **12a–c**.

120° dendritic donors and 120° ferrocenyl acceptors resulted in hexagonal, hexafunctionnalized metallocycles **12a–c** (Scheme 2).[21d] Their cyclic voltammograms reveal a unique redox wave corresponding to the reversible oxidation of the Fc units. Again, the authors could extract the values of the diffusion coefficients *D* from the CV experiments with, as expected, decreasing values when increasing the molecular weight.

A step further lies on the extension of this strategy from metalla-rings bearing Fc units to analogous 3D metalla-cages.[22] The cuboctahedral complex **13** (Scheme 3) was obtained from a 120° Fc acceptor complex and a tritopic pyridyl ligand. Its redox properties were explored in detail. Each Fc unit exhibits a similar half-wave potential and no decomposition of the assembly is observed during the redox process. The *D* values extracted from the electrochemical measurements are similar to those obtained from the DOSY NMR experiment. Remarkably, the corresponding external diameter calculated from the Stokes-Einstein[23] equation (6.7 nm) is close to the value obtained from the molecular force field model structure (6.9 nm). Finally, the diffusion coefficient allows assessing of the presence of twelve redox units on the metalla-cage, indicating that all the ferrocenyl moieties are oxidized simultaneously. In addition to these self-assembled rings and cages decorated with pendant redox active Fc units, P. J. Stang and coworkers described a rectangular assembly **14** which incorporates the Fc moiety as a constituting part of the ring skeleton (Fig. 7a).[24] The electronic properties of **14** were studied by cyclic voltammetry (Fig. 7b) and show two reversible waves at E = +0.12 and +0.33 V *vs.* Fc/Fc$^+$. The first redox process was assigned to a two-electron exchange centered on both Fc units and the second one, to the simultaneous oxidation of anthracenyl units. Interestingly, the

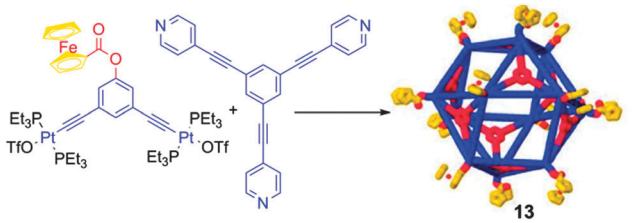

Scheme 3 Synthesis of cuboctahedral assembly **13**.

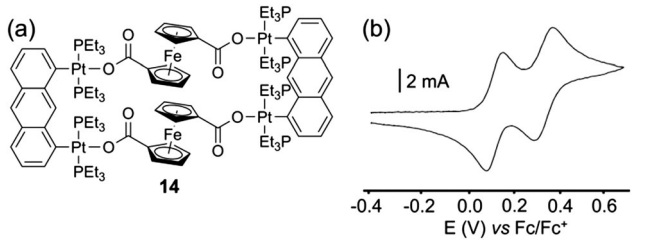

Fig. 7 (a) Rectangular assembly **14**; (b) cyclic voltammogram of **14**: CH_2Cl_2 (Bu_4NPF_6 (0.1 M)), scan rate 200 mV s^{-1}.

authors could determine from the spectroelectrochemical analysis that the intermediate $\mathbf{14}^{2+}$ coexists in equilibrium with the neutral and the tetracationic forms.

Rings and cages incorporating the tetrathiafulvalene core

The tetrathiafulvalene (TTF) moiety has received a great deal of attention as a key building block in the preparation of conducting and semiconducting materials.[25] Its remarkable electrochemical behaviour is characterized by two reversible oxidation steps at low potentials, which produce stable oxidized species $TTF^{\bullet+}$ and TTF^{2+}. This property has promoted this unit to a key building block for the elaboration of numerous molecular and supramolecular switchable systems.[26] Besides offering an extra redox state compared to ferrocene, another key issue for TTF lies on its planar π-conjugated geometry. Therefore, unlike ferrocene, TTF and its derivatives can constitute themselves the side walls of the cavity upon a self-assembly process, giving rise to metalla-rings or -cages endowed with electron rich internal cavities.

J.-L. Zuo and coworkers described neutral complexes **15** and **16** (Fig. 8a).[27] The latter was obtained in one step by the reaction of a mixture of *cis* and *trans* bis(pyrazole)-TTF ligands with $Re(CO)_5Cl$. Their XRD analysis revealed that the TTF skeleton is bended in **15** and planar in metalla-ring **16**. The high geometric constraints occurring in such small size self-assembled systems have of course a strong impact on the electronic integrity of the TTF unit (Fig. 8b). In both cases, the usual well-defined two-step redox behaviour of TTF cannot be recovered, due to the strong geometric constraint applied to the TTF core upon oxidation in the case of **15** and to an electronic coupling between the facing TTF redox units in the case of **16**.

Another metalla-ring involving a metal carbonyl complex and a TTF derivative, namely vinylogous tetrathiafulvalene (TTFV), was described by D. Lorcy and coworkers (Fig. 8c).[28] The latter is constructed from the self-assembly of a non-planar bispyridyl TTFV ligand with hexacarbonyl molybdenum in a 1 : 1 molar ratio. The electrochemical properties of metalla-square **17** which incorporates four redox-active units were studied by cyclic voltammetry. The system appears to be oxidized according to two successive processes at E = +0.48 and +0.74 V *vs.* SCE. The first one is attributed to the 0/•+ oxidation of the organic part, which is slightly shifted compared to the TTFV ligand precursor, the second wave being ascribed to the superimposition of both metal center oxidation with the •+/2+ ligand centered oxidation.

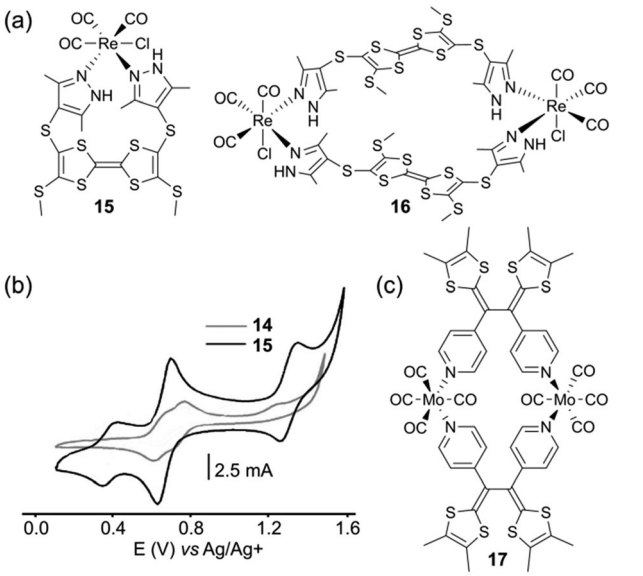

Fig. 8 (a) Assemblies **15** and **16**; (b) cyclic voltammograms of **15** and **16**: C = 0.5 mM in CH_2Cl_2 (Bu_4NClO_4), scan rate 100 mV s^{-1}; (c) assembly **17**.

In the course of the studies conducted at Angers, related to the synthesis of electron-rich supramolecular discrete systems, we described recently several examples of metalla-rings and -cages whose cavities are made from TTF or its derivatives. For this purpose, several di- and tetra-topic ligands either designed from the parent TTF skeleton (**18**) or two of its well-known derivatives, namely bis(pyrollo)TTF (BPTTF)[29] (**19**, **20**) and the so-called extended-TTF (exTTF)[30] (**21**) were synthesized (Scheme 4).

As a common feature, all of these ligands integrate a central sulfur-rich electron-rich framework. The first example of a metal-driven self-assembled system issued from the parent TTF corresponds to the octanuclear metalla-cage **22**, which was prepared in collaboration with B. Therrien and colleagues (Fig. 9a). Reaction between tetratopic ligand **18** and dinuclear *p*-cymene oxalato ruthenium acceptor **Ru1** afforded metalla-cube **22**, whereas the reaction with dinuclear *p*-cymene quinonato complex **Ru2** afforded tetranuclear plate **23**.[31] The selective

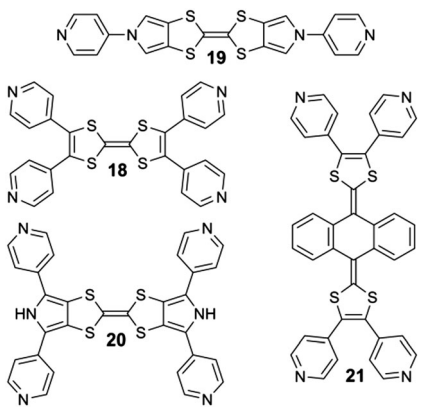

Scheme 4 Di- and tetra-topic TTF-based ligands **18**, **19**, **20** and **21** prepared at Angers.

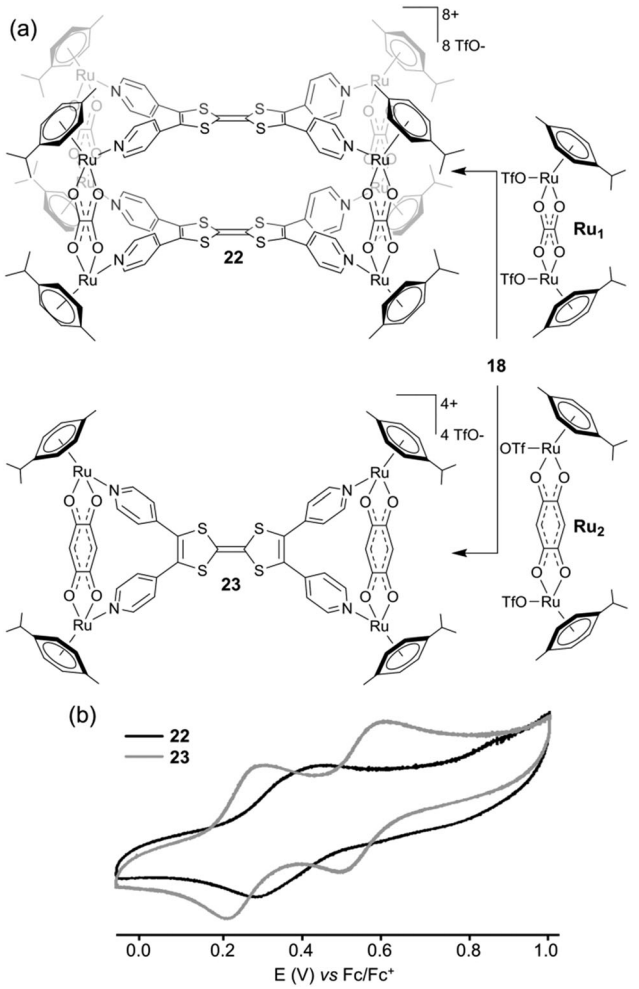

Fig. 9 (a) Synthesis of metalla-cage **22** and metalla-plate **23**; (b) cyclic voltammogram of **22** and **23**: C = 0.5 mM in CH_3CN (Bu_4NPF_6 (0.1 M)), scan rate 50 mV s^{-1}.

formation of these two different architectures results from geometrical complementary interactions between **18** and the respective **Ru1** and **Ru2** counterparts. Two pyridyl nitrogen atoms located on the same dithiol unit in ligand **18** are separated by 6.7 Å, whereas both ruthenium centers are at a distance of 5.5 Å in complex **Ru1** and at 7.9 Å in complex **Ru2**. Therefore, the good size matching between ligand **18** and **Ru2** affords tetranuclear plate **23** whereas the smaller ruthenium acceptor **Ru1** generates cage **22**. Both assemblies were studied by cyclic voltammetry (Fig. 9b). Two characteristic redox waves corresponding to the TTF moiety are observed in plate **23** (E = +0.28 and +0.58 V *vs.* Fc/Fc^+), shifted to higher potential in comparison to ligand **18** (E = +0.22 and +0.55 V *vs.* Fc/Fc^+) as a consequence of the coordination to the metal centers. The electrochemical behaviour observed for metalla-cage **22** is significantly different since only one oxidation wave is observed, at E = +0.44 V *vs.* Fc/Fc^+. This peculiar behaviour is assigned to the rigidity of the metalla-assembly which may alter the kinetics associated with the conformational changes which usually occur upon the electrochemical oxidation of TTF derivatives. It is indeed well-established that the TTF parent system undergoes severe conformational changes upon oxidation to heteroaromatic 1,3-dithiolium cations $TTF^{\bullet+}$ and TTF^{2+}. Whereas neutral TTF corresponds to a distorded boat-like structure, $TTF^{\bullet+}$ is planar and TTF^{2+} is significantly twisted around the central C–C bond.[25a,32] Consequently, if structural elements located on the periphery of the TTF skeleton prevent those conformational changes upon oxidation, the usual well-defined reversible two-step redox behaviour of TTF is not observed anymore. This is observed for instance with geometrically constrained tetrathiafulvalenophanes[33] or TTF-based cage molecules,[34] and is also observed in the case of metalla-cage **22**. Another family of electro-active discrete self-assembled cages could be synthesized from ligand **18**. The reaction of the latter with *cis*-blocked Pd(II) or Pt(II) complexes (*i.e. cis*-M(dppf)$(OTf)_2$; dppf = 1,1′-bis(diphenylphosphino)ferrocene; OTf = trifluoromethane-sulfonate) in a 1 : 2 molar ratio afforded metalla-architectures **24a** (Pt) or **24b** (Pd).[35] Both present an estimated hydrodynamic radii of *ca.* 16 Å as extracted from DOSY NMR experiments which, in addition to other spectroscopic data, well agrees with a M_8L_4 cubic geometry (Fig. 10a). Cyclic voltammetry experiments conducted on metalla-cages **24a** and **24b** show three reversible redox processes. Two are assigned to the TTF side walls and the third one to the corner ferrocene units. Interestingly, the latter can be used as an internal reference to address the number of electrons exchanged. The relative peak intensities of the three systems (*i.e.* 1/1/2) observed from the deconvoluted cyclic voltammogram (Fig. 10b) agree with two successive independent oxidations of the four TTF units at E = +0.30 and +0.60 V and of the eight ferrocenes at E = +0.80 V *vs.* Fc/Fc^+, giving rise in total, to the reversible generation of sixteen positive charges on the periphery

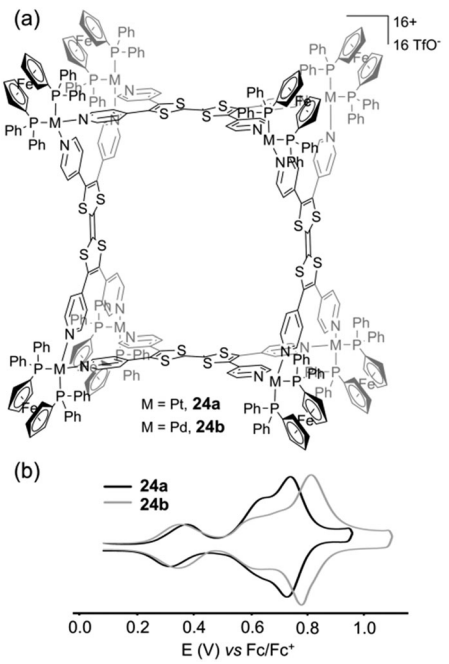

Fig. 10 (a) Cubic assemblies **24a** and **24b**; (b) deconvoluted cyclic voltammogram of **24a** and **24b**: C = 0.5 mM in CH_3CN (Bu_4NPF_6 (0.1 M)), scan rate 20 mV s^{-1}.

of the cavity. Molecular squares prepared by the coordination-driven self-assembly strategy are typically issued from the interaction between a linear ditopic ligand and a *cis*-blocked square planar metallic center. Depending on the length of the linear ligand or on its flexibility, the reaction can also lead to triangular systems beside the molecular square, both polygons being usually difficult to separate. Thus, the reaction of the linear *N*,*N*′-dipyridyl-(BPTTF) ligand[36] **19** with an equimolar ratio of *cis*-Pt(dppp)$(OTf)_2$, (dppp = 1,3-bis(diphenylphosphino)propane), produces a mixture of triangle **25** and square **26** (Fig. 11a). Remarkably, in this case, each polygon could be easily isolated by selective precipitation.[37] Both metalla-rings **25** and **26** were fully characterized by different methods.

Noteworthy, the ratio between their respective experimental radii ($R_{triangle}/R_{square}$) extracted from DOSY NMR reaches a value of 0.80, in excellent agreement with the theoretical value. As usually observed for BPTTF derivatives, triangle **25** and square **26** exhibit two reversible oxidation waves (E = +0.70 and +1.00 V *vs.* Fc/Fc^+) (Fig. 11b). In order to address the number of electrons exchanged in each process, ferrocene was added to the electrochemical solutions and used as an internal coulometric reference (*i.e.* three equivalents for triangle **25** and four equivalents for square **26**). Analysis of the resulting respective peak intensities from the deconvoluted CV (Fig. 11b) suggests that the BPTTF side walls behave independently and that the metalla-rings are fully oxidized to their respective $\mathbf{25}^{6+}$ and $\mathbf{26}^{8+}$ stable states. Given the π-donating character of BPTTF derivatives, a peculiar feature of such polygons lies on the strong electronic density which is spread over the walls of the cavity, which in principle is favourable to bind to a complementary electron-poor guest within the cavity. On the other hand, the preparation of molecular and supramolecular hosts able to bind fullerene derivatives is a subject of intense interest.[38] In this context, the binding affinity of **25** and **26** for electro-deficient C_{60} or C_{70} was monitored by UV-Vis titrations. The titration spectra as well as a Job's plot analysis (Fig. 11c) demonstrate a good binding affinity of triangle **25** for C_{60} (or C_{70}) in a 1 : 1 stoichiometry. This result is supported by a good electronic complementarity of both components as well as by a suitable size matching between the cavity of **25** and a fullerene guest. The latter property is not satisfied in the case of square **26** whose cavity is much larger and which indeed does not exhibit any affinity for those fullerenes in UV-vis titration experiments.

With the aim to switch from electron-rich metalla-rings to metalla-cages, the tetratopic BPTTF-based ligand **20** (Scheme 4) was designed. The latter was reacted with square planar *cis*-$Pt(PEt_3)_2(OTf)_2$ complex and the reaction converged in less than two hours into a single discrete prismatic cage **27** (Fig. 12a).[39] The M_6L_3 formula was confirmed by ESI-MS mass spectroscopy and by an X-ray diffraction experiment (Fig. 12b). Cyclic voltammetry of

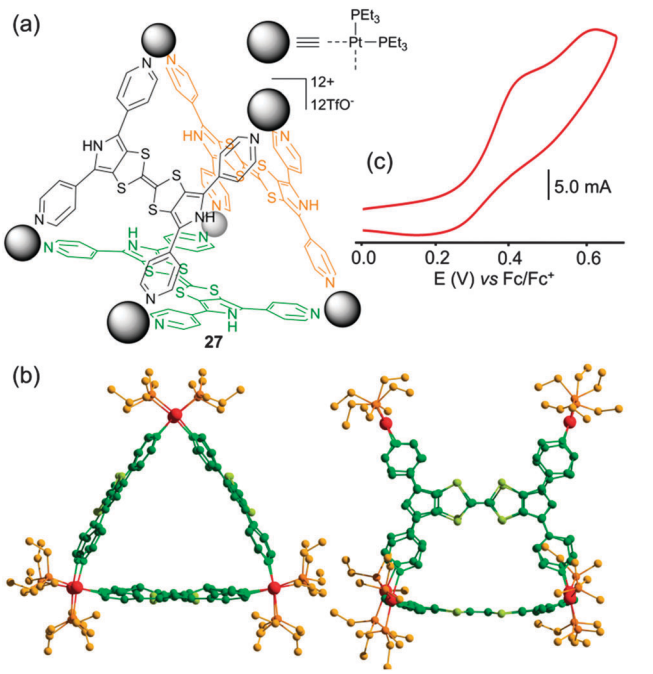

Fig. 12 (a) Metalla-prism **27**; (b) X-ray crystal structure of **27**; (c) cyclic voltammogram of **27**: C = 0.6 mM in CH_3CN (Bu_4NPF_6 (0.1 M)), scan rate 50 mV s^{-1}.

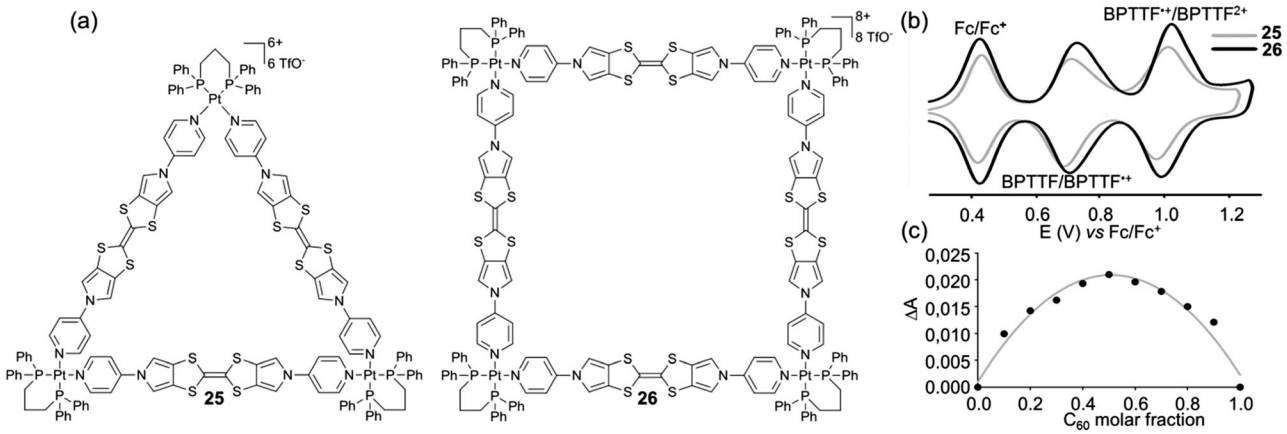

Fig. 11 (a) Triangle **25** and square **26**; (b) deconvoluted cyclic voltammogram of **25** and **26** in the presence of ferrocene (3.0 and 4.0 equiv. respectively): C = 0.5 mM in CH_3CN (Bu_4NPF_6 (0.1 M)), scan rate 20 mV s^{-1}; (c) Job's plot at 407 nm, triangle **25** *vs.* C_{60} ($C = 1.3 \times 10^{-5}$ M in CS_2/CH_2Cl_2 (4/1)).

metalla-cage **27** (Fig. 12c) reveals the presence of two successive oxidation waves, located at fairly low potentials (E = +0.43 and +0.62 V *vs.* Fc/Fc^+) but poorly reversible due to a combination of steric and electronic factors. The guest binding capability of prism **27** was studied by UV-Vis spectroscopy with an electro-deficient compound (TCNQ-F_4). The progressive addition of the guest to a solution of electron-rich M_6L_3 cage **27** leads to the formation of an inclusion complex with a 1:1 stoichiometry as extracted from a Job's plot analysis.

A third family of discrete metalla-assemblies that we have been developing[40] is based on the exTTF framework. This π-donating skeleton exhibits unique electronic and geometrical properties that have been widely explored by N. Martín and coworkers in the construction of covalent hosts prone to encapsulate electro-deficient fullerene guests.[38a]

On this basis, tetrapyridyl-exTTF ligand **21** (Scheme 4) was synthesized in one step from pristine exTTF through a palladium catalyzed C–H arylation. A mixture of ligand **21** and *cis*-Pd(dppf)$(OTf)_2$ in a 1:2 molar ratio afforded in only five minutes one discrete assembly **28a** (Fig. 13a).[40] Both species, ligand **21** and resulting M_4L_2 assembly **28a** (Fig. 13b) could be characterized by X-ray diffraction. Ligand **21** displays the usual exTTF butterfly shape with a 86° dihedral angle between both 1,3-dithiol-2-ylidene mean plans. This curvature is amplified in the M_4L_2 container **28a** with a dihedral angle of 56° which gives rise to an ovoid cavity whose size and shape are suitable for the inclusion of a planar guest. In particular, the formation of a 1:1 host–guest inclusion complex with perylene ($K_a \approx 3.9 \times 10^3$) could be demonstrated by ^{1}H NMR, DOSY NMR and ESI-FTICR. Electrochemical properties of ligand **21** and container **28a** were studied by cyclic voltammetry (Fig. 13c). In addition to a first oxidation wave attributed to the two-electron oxidation steps of each exTTF scaffold (E = +0.57 V *vs.* Fc/Fc^+), container **28a** exhibits a second oxidation process centered on the four ferrocene units (E = +0.80 V). Compared to ligand **21**, the oxidation of exTTF in the complex is shifted to higher potentials due to the coordination to the metal center and appears irreversible presumably because of the rigidity of the self-assembly which prevents redox-driven conformational changes which usually occur with exTTF derivatives.

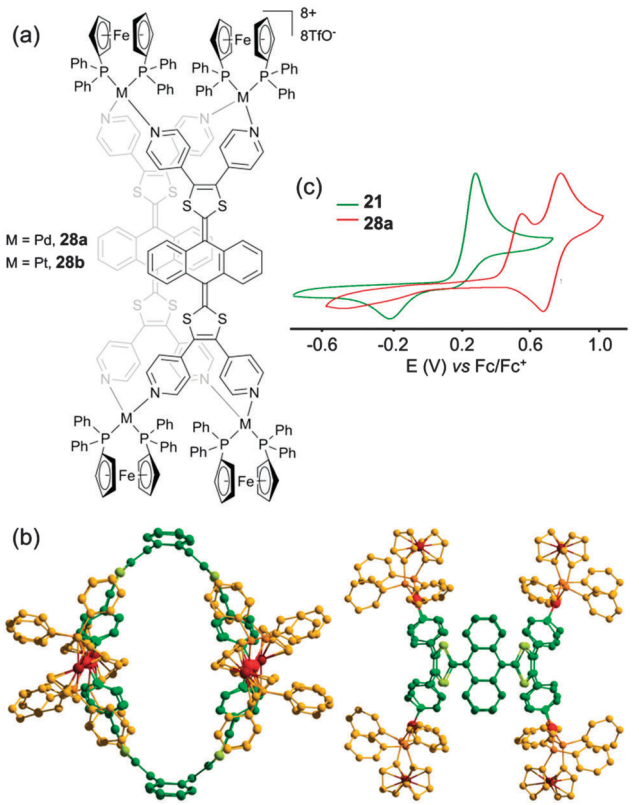

Fig. 13 (a) Metalla-assemblies **28a** and **28b**; (b) X-ray crystal structure of cage **28a**; (c) cyclic voltammogram of ligand **21** and cage **28a**: C = 1.0 mM in CH_3CN/CH_2Cl_2 (1/1) (**21**) or CH_3CN (**28a**) (Bu_4NPF_6 (0.1 M)), scan rate 100 mV s^{-1}.

Miscellaneous

Self-assembled polygons/polyhedra are prepared from complementary ligands and metal complexes and the redox activity of the resulting assemblies is closely linked to the electroactivity of each partner. Basically, the redox character of the metalla-ring/cage can be mainly localized on the cavity walls (in general the ligand) as shown above through various examples, or on the corner (in general the metal), or on both partners. In the latter case, the ligand and the metal can behave independently or are sometimes electronically coupled as shown through some examples above.

A promising development of self-assembled metalla-cages concerns their use as anti-cancer agents.[1a,t,41] Based on the fact that various Ru(III) and arene Ru(II) complexes exhibit interesting cytotoxic effects, B. Therrien and colleagues have developed several families of water soluble cationic metalla-cages constructed from arene ruthenium complexes.[1t,41a,c] The authors have demonstrated the efficiency of such assemblies for increasing the solubility and cell permeability of drug-like molecules or photodynamic therapy (PDT) agents. Some of these metalla-assemblies were electrochemically studied. An illustrative example is given with the tetranuclear metalla-rectangle **29** (Fig. 14a),[42] which is obtained from the reaction of a bipyridine ligand with a dinuclear arene ruthenium complex for which two Ru centers are bridged by a 1,4-benzoquinonato moiety. The redox properties of metalla-rectangle **29** have been studied by cyclic voltammetry (Fig. 14b). Compared to the dinuclear arene ruthenium precursor **Ru2**, rectangle **29** appears much easier to reduce, due to the presence of four positive charges in the metalla-assembly. Rectangle **29** undergoes three successive reduction waves at E = −0.68 (reversible, *vs.* Fc/Fc^+), −1.39 (irr.) and −1.90 V (irr.) and no oxidation could be detected before electrolyte decomposition. Though the ligand orbitals are closely mixed with metal-based ones, these reduction processes can formally be assigned to electron injection occurring predominantly onto the quinonato bridging ligand.

A similar electrochemical behaviour (Fig. 14c) could be observed by P. Mukherjee and colleagues, from a 3D macrocyclic cage **30** (Fig. 14a) featuring the same bis-bidentate

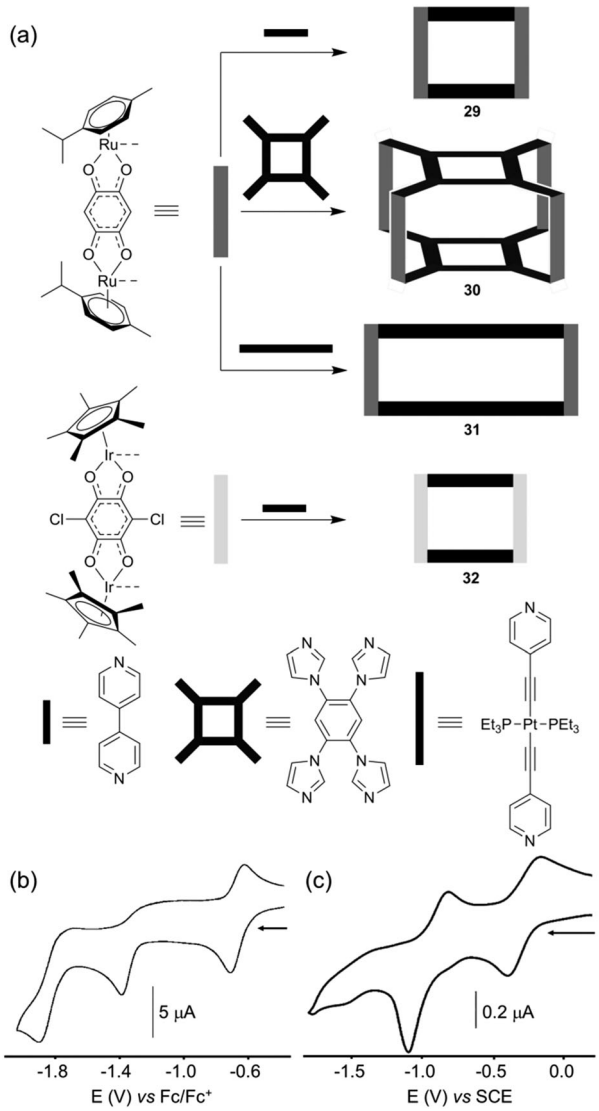

Fig. 14 (a) Schematic representation and synthesis of metalla-assemblies **29–32**; cyclic voltammogram of **29** (b) and **30** (c): (b) C = 0.5 mM in CH_2Cl_2 (Bu_4NPF_6 (0.1 M)), scan rate 100 mV s^{-1}; (c) CH_2Cl_2 (NBu_4PF_6 (0.1 M)), scan rate 100 mV s^{-1}.

quinonato Ru complex **Ru2**, which is associated in this case with a tetra-imidazole ligand.[43] Note that 2D analogous assemblies based on bis-imidazole ligands were also electrochemically characterized.[44] Finally, the highly modular character of the stepwise strategy using half-sandwich piano-stool complexes for the construction of discrete electroactive polygons is illustrated by the possibility to change either the bridging dipyridyl ligand to a longer one as in rectangle **31**,[45] or the metal as in **32** which integrates an iridium metal complex instead of a ruthenium one.[1q,46]

Beyond Ru-based cages and as mentioned above with the encapsulation of a Pt(IV) prodrug **AdPt**,[9] metalla-cages incorporating square planar Pt(II) and Pd(II) complexes have also been used as drug delivery vectors. This is the case with metalla-cages **33a–d** recently described by J. D. Crowley and colleagues (Scheme 5a) which integrate a variety of functional groups on the outer surface of the host cage. They were prepared according to a very efficient modular approach based on the CuAAC 'click' reaction.[47] Using this strategy, various functions were appended on the periphery of the cage, some being redox-active. The cyclic voltammetry study of compounds **33a–d** in DMF shows basically a superposition of the redox contribution of each electroactive partner, be they reducible or oxidable. They display irreversible reductions at negative potentials (*ca.* E = −1.7 and −1.9 V *vs.* Fc*/Fc*$^+$) assigned to the 2,6-bis(ethynyl)pyridine ligand framework as well as redox processes corresponding to the appended functional groups. In particular, the ferrocenyl-substituted cage **33a** displays the usual reversible oxidation process of ferrocene at E = +0.5 V *vs.* Fc*/Fc*$^+$ and no electronic communication was observed between the four pendant Fc units, as expected from their large spatial separation.

With a similar objective to decorate the outer surface of a metalla-structure, R. Yang *et al.* described the $M_{12}L_{24}$ sphere **34** (Scheme 5b) which integrates 24 thiophene units.[48] The investigation of the electrochemical properties of **34** in DMSO is characterized by a reduction process at E = −1.06 V *vs.* Ag/AgCl. No information is provided regarding the oxidation and electropolymerization ability of this thiophene-rich system.

The case of square **35** (Scheme 6) depicted by A. J. Lees and colleagues[49] is interesting since it encompasses three redox active centers, *i.e.* Ru(II)/Ru(III), Fc/Fc$^+$ and the terpyridine ligand, all of them behaving independently. Two oxidation

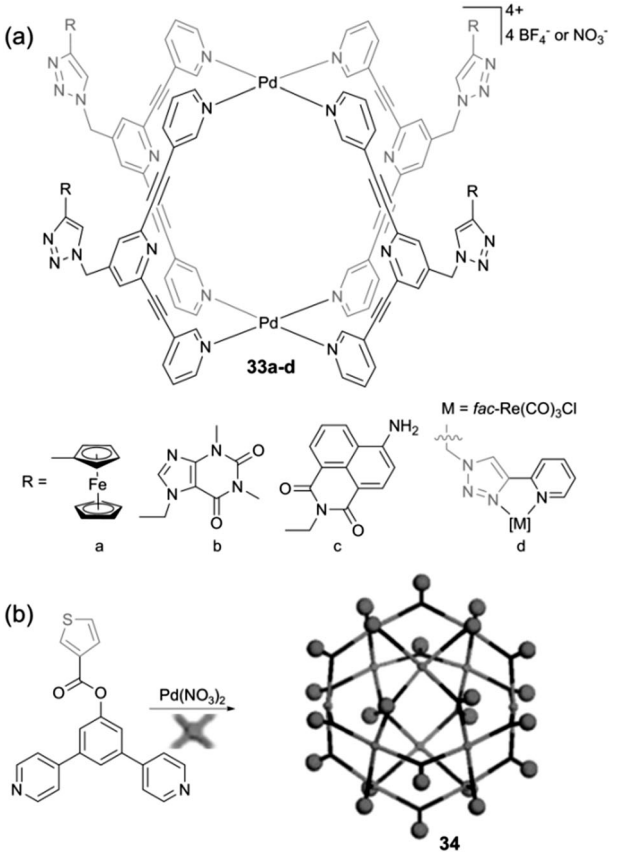

Scheme 5 Metalla-assemblies **33a–d** and **34**.

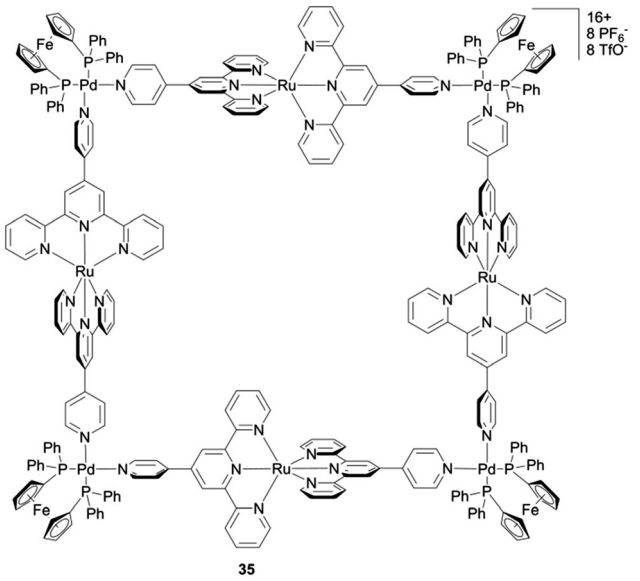

Scheme 6 Metalla-square **35**.

waves are observed and assigned to the Ru(II)/Ru(III) (E = +0.70 V *vs.* Fc/Fc^+) and to the Fc corner (E = +0.88 V) respectively, whereas the reduction of the terpyridine fragment gives rise to two successive reduction processes. The comparison of the electrochemical behaviour of cyclen Ru-based triangle **36** and square **37** (Fig. 15a) described by J. R. Long and coworkers, provides an interesting case for using the electrochemistry tool in probing a molecular structure.[50] Unlike triangle **25** and square **26** presented above and which exhibit similar cyclic voltammograms, quite different ones are observed for the triangular $(cyclen)_3[Ru_3(4,4'\text{-bpy})_3](PF_6)_6$ **36** and the square $(cyclen)_4[Ru_4\text{-}(4,4'\text{-bpy})_4](OTf)_8$ **37**. The former is oxidized following three distinct redox processes at E = +0.23, +0.37 and +0.48 V *vs.* Fc/Fc^+ in acetonitrile, each of them corresponding to a Ru-centered one-electron exchange, whereas square **37** exhibits one single reversible four-electron process at E = +0.48 V and a high scan rate (1000 mV s^{-1}). This difference is assigned to the more sterically constrained structure in the case of the triangle, which prevents any rotation of the pyridine rings with respect to each other and which favours electronic coupling by delocalization. Such a difference between homologous polygons nicely illustrates how the geometry of molecules built from the same components can have a direct impact on their electrochemical properties.

Because of their unusual topology and as illustrated with **36**, metalla-triangles are appealing for the study of their redox properties. Another relevant example corresponds to Ru-based triangles **38a,b** built from adenine ligands (Fig. 16). These metalla-rings, depicted by J. A. Thomas and coworkers,[51] display a well-defined reversible electrochemical behaviour which is manifested by three Ru-based reversible oxidation processes, from which the authors could demonstrate the occurrence of two discernible mixed-valence states.

The case of the phenothiazine heterocycle is interesting since this system can be reversibly oxidized into a radical-cation at E = +0.73 V *vs.* SCE (acetonitrile) with the possibility of further oxidation or disproportionation. This favourable

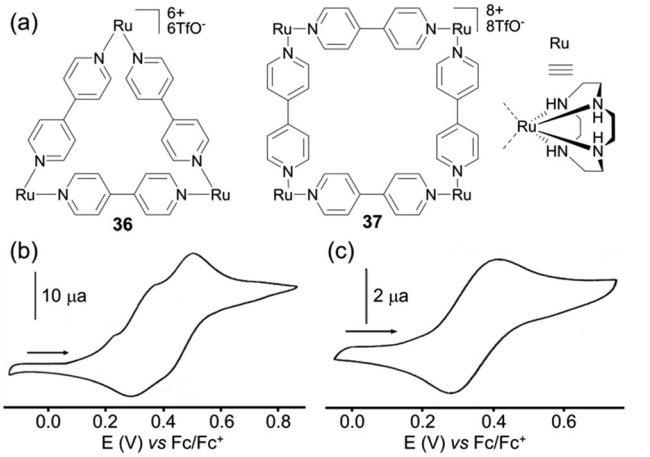

Fig. 15 (a) Metalla-triangle **36** and metalla-square **37**; cyclic voltammograms of **36** (b) and **37** (c), C = 1 mM in CH_3CN (Bu_4NPF_6 (0.1 M)), scan rate 100 mV s^{-1} (b) and (Bu_4NClO_4 (0.1 M)), scan rate 1000 mV s^{-1} (c).

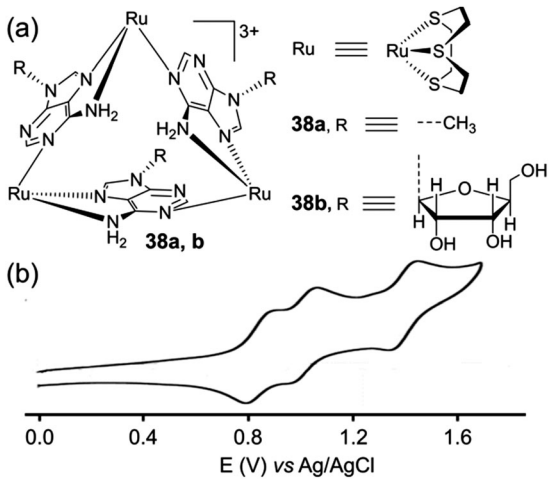

Fig. 16 (a) Metalla-triangle **38a–b**; (b) cyclic voltammograms of **38a**, CH_3CN (Bu_4NPF_6 (0.1 M)).

redox behaviour prompted G. H. Clever and colleagues to describe recently a phenothiazine-based coordination cage **39a**.[1c,52] The latter corresponds to an interpenetrated double cage based on eight phenothiazine ligands and four square-planar-coordinated Pd(II) cations (Fig. 17). Remarkably, the corresponding *S*-monooxygenated sulfoxyde and *S*-dioxygenated sulfone cages **39b** and **39c** could be successively obtained from **39a** through a stepwise chemical oxidation with $Cu(NO_3)_2{\cdot}3H_2O$ or, in the case of **39b**, upon standing in air for two months. The three double cages **39a–c** exhibit significant different shapes in the solid state as shown by their respective X-ray diffraction structures (Fig. 17b–d).[52,53] Interestingly, titration with the oxidant $[Fe(III)(bipyridine)_3]^{3+}$, followed by reaction with water, shows that the intermediate cation radical $\mathbf{39a}^{8\bullet+}$ reacts much faster with water compared to the cation-radical generated from the phenothiazine ligand precursor. This is ascribed to a cage effect which, upon oxidation, favours an intramolecular disproportionation. This property results in neutral and dicationic phenothiazine facets in the double cage, the latter

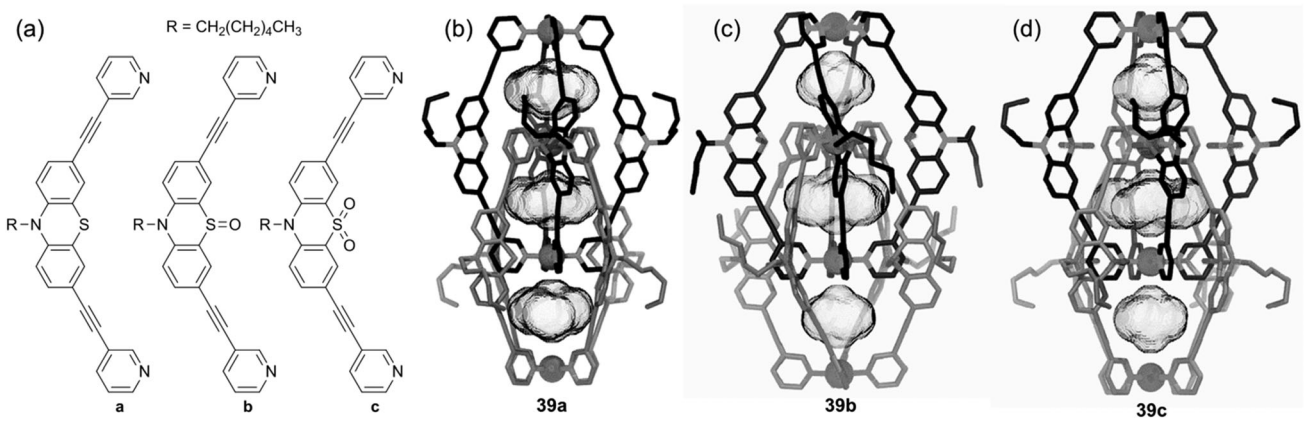

Fig. 17 X-ray single-crystal structures of double cages **39a** (b), **39b** (c), **39c** (d) (Metal = Palladium) and their corresponding constitutive ligands (a).

dications being known intermediates in the production of *S*-monooxygenated sulfoxyde upon reaction with water. Finally, an interesting case concerns metalla-rectangle **40** described by C. N. Hsu and colleagues[54] This tetranuclear iron thiolate complex can be electrochemically reduced according to three successive reversible redox processes ($E = -0.28$, -0.84 and -0.93 V *vs.* Fc/Fc^{+}) (Fig. 18). It appears that in this rectangle, the 1,4-diisocyanobenzene ligand does not assist the electron communication between both iron thiolate cores, which behave independently at the first two-electron redox process ($\mathbf{40}^{4+}/\mathbf{40}^{2+}$). The second and third processes are assigned to two one-electron exchanges corresponding to $\mathbf{40}^{2+}/\mathbf{40}^{+}$ and $\mathbf{40}^{+}/\mathbf{40}^{0}$ couples respectively, redox states for which a weak exchange interaction seems to occur through the 1,4-diisocyanobenzene ligand. The most striking feature of this system, which could be demonstrated thanks to the single-crystal X-ray structures of $\mathbf{40}^{4+}$ and $\mathbf{40}^{2+}$, comes from their different cavity size, which appears larger in the tetracationic form than in the reduced one. Therefore, this work provides a nice illustration of how the size of a self-assembled redox-active system can be controlled thanks to a redox stimulus, opening therefore interesting perspectives in terms of electrochemical-triggering of guest binding.

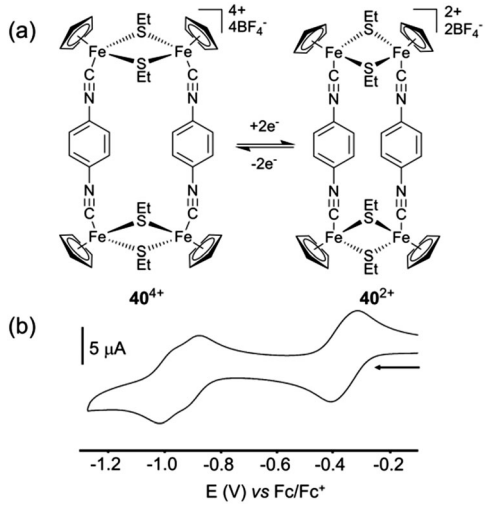

Fig. 18 (a) Redox-controlled cavity modulation of rectangular complex **40**; (b) cyclic voltammogram of **40**: C = 0.2 mM in CH_3CN (Bu_4NPF_6 (0.1 M)), scan rate 100 mV s^{-1}.

Conclusions and outlooks

Thanks to the synthetic efficiency and to the modular character of the self-assembly approach, a wide diversity of discrete redox-rings/cages have been made available during the last decade. This diversity is supported by the cumulated inherent structural and electronic characteristics of the starting building blocks, *i.e.* ligands and metal complexes or can also result from synergetic effects between both components. The latter can be electronically coupled or not, giving rise to a large panoply of reducible or oxidable discrete cavities which differ in the structure or in the function. From this point of view, and as shown through various examples in this article, a key issue of such redox-active systems relies on the possibility to fine tune the charge state of the cavity, be it positive or negative, by a simple control over the applied electrical potential or of the oxidizing/reducing chemical agent. On this ground, it is worth mentioning that beyond potential applications in electrochemical sensing for environmental and medical sciences[4,55] or for redox catalysis,[1i] a valuable extension of such control over the cavity charge lies in the possibility to trigger: (i) the cavity size, as in the case of metalla-rectangle **40**,[54] (ii) the binding affinity between the redox-active host cavity and a given guest, a key issue for delivery applications. From this point of view, the possibility to trigger the host–guest affinity, thanks to an external physical stimulus, is the subject of intense interest. Promising results have been already obtained for discrete self-assembled host cavities, as for example in the case of light-switchable metalla-cages.[1c,3] Chemical stimuli such as addition of a competing ligand or the use of pH-sensitive components[56] have also been used successfully. On the other hand, redox-stimuli are able to tune the charge state of the host cavity, that is, its ionic level, which attracts a strong interest. Such a system should allow in principle to bind, or conversely to expel the guest, simply by modifying the electrostatic host–guest interactions. This concept has already been demonstrated for

instance with a molecular organocyanometalate box which permits a redox-switch of the complexation/decomplexation process of K^+ and Cs^+.[57] Given the tremendous advances recently achieved regarding the design of new highly functionalized redox-responsive self-assembled hosts, promising perspectives are therefore offered for extending this concept to the binding control of various guests of interest, be they ionic or neutral.

Acknowledgements

The authors gratefully acknowledge the MENRT for a PhD grant (VC).

Notes and references

1 For recent reviews, see: (*a*) N. Ahmad, H. A. Younus, A. H. Chughtai and F. Verpoort, *Chem. Soc. Rev.*, 2015, **44**, 9; (*b*) S. Zarra, D. M. Wood, D. A. Roberts and J. R. Nitschke, *Chem. Soc. Rev.*, 2015, **44**, 419; (*c*) M. Han, D. M. Engelhard and G. H. Clever, *Chem. Soc. Rev.*, 2014, **43**, 1848; (*d*) S. Mukherjee and P. S. Mukherjee, *Chem. Commun.*, 2014, **50**, 2239; (*e*) T. R. Cook, V. Vajpayee, M. H. Lee, P. J. Stang and K.-W. Chi, *Acc. Chem. Res.*, 2013, **46**, 2464; (*f*) K. Harris, D. Fujita and M. Fujita, *Chem. Commun.*, 2013, **49**, 6703; (*g*) A. Mishra, S. C. Kang and K.-W. Chi, *Eur. J. Inorg. Chem.*, 2013, 5222; (*h*) M. M. J. Smulders, I. A. Riddell, C. Browne and J. R. Nitschke, *Chem. Soc. Rev.*, 2013, **42**, 1728; (*i*) M. D. Ward and P. R. Raithby, *Chem. Soc. Rev.*, 2013, **42**, 1619; (*j*) H. Amouri, C. Desmarets and J. Moussa, *Chem. Rev.*, 2012, **112**, 2015; (*k*) T. R. Cook, Y.-R. Zheng and P. J. Stang, *Chem. Rev.*, 2012, **113**, 734; (*l*) L. R. MacGillivray, *Angew. Chem., Int. Ed.*, 2012, **51**, 1110; (*m*) R. Chakrabarty, P. S. Mukherjee and P. J. Stang, *Chem. Rev.*, 2011, **111**, 6810; (*n*) Y. Inokuma, M. Kawano and M. Fujita, *Nat. Chem.*, 2011, **3**, 349; (*o*) S. De, K. Mahata and M. Schmittel, *Chem. Soc. Rev.*, 2010, **39**, 1555; (*p*) P. Jin, S. J. Dalgarno and J. L. Atwood, *Coord. Chem. Rev.*, 2010, **254**, 1760; (*q*) Y.-F. Han, W.-G. Jia, W.-B. Yu and G.-X. Jin, *Chem. Soc. Rev.*, 2009, **38**, 3419; (*r*) B. H. Northrop, Y.-R. Zheng, K.-W. Chi and P. J. Stang, *Acc. Chem. Res.*, 2009, **42**, 1554; (*s*) P. J. Stang, *J. Org. Chem.*, 2009, **74**, 2; (*t*) B. Therrien, *Eur. J. Inorg. Chem.*, 2009, 2445; (*u*) M. Yoshizawa, J. K. Klosterman and M. Fujita, *Angew. Chem., Int. Ed.*, 2009, **48**, 3418; (*v*) M. W. Cooke, D. Chartrand and G. S. Hanan, *Coord. Chem. Rev.*, 2008, **252**, 903; (*w*) S. J. Dalgarno, N. P. Power and J. L. Atwood, *Coord. Chem. Rev.*, 2008, **252**, 825; (*x*) B. H. Northrop, D. Chercka and P. J. Stang, *Tetrahedron*, 2008, **64**, 11495; (*y*) B. H. Northrop, H. B. Yang and P. J. Stang, *Chem. Commun.*, 2008, 5896; (*z*) E. Zangrando, M. Casanova and E. Alessio, *Chem. Rev.*, 2008, **108**, 4979.

2 (*a*) C. H. Amijs, G. P. van Klink and G. van Koten, *Dalton Trans.*, 2006, 308; (*b*) F. Wurthner, C.-C. You and C. R. Saha-Moller, *Chem. Soc. Rev.*, 2004, **33**, 133.

3 (*a*) M. Han, R. Michel, B. He, Y. S. Chen, D. Stalke, M. John and G. H. Clever, *Angew. Chem., Int. Ed.*, 2013, **52**, 1319; (*b*) T. Murase, S. Sato and M. Fujita, *Angew. Chem., Int. Ed.*, 2007, **46**, 5133.

4 S. Goeb, D. Canevet and M. Sallé, *Organic Synthesis and Molecular Engineering*, John Wiley & Sons, Inc., 2013, p. 213.

5 S. T. Schneebeli, M. Frasconi, Z. Liu, Y. Wu, D. M. Gardner, N. L. Strutt, C. Cheng, R. Carmieli, M. R. Wasielewski and J. F. Stoddart, *Angew. Chem., Int. Ed.*, 2013, **52**, 13100.

6 (*a*) M. Fujita, D. Oguro, M. Miyazawa, H. Oka, K. Yamaguchi and K. Ogura, *Nature*, 1995, **378**, 469; (*b*) M. Fujita, K. Umemoto, M. Yoshizawa, N. Fujita, T. Kusukawa and K. Biradha, *Chem. Commun.*, 2001, 509.

7 Y. Furutani, H. Kandori, M. Kawano, K. Nakabayashi, M. Yoshizawa and M. Fujita, *J. Am. Chem. Soc.*, 2009, **131**, 4764.

8 M. Yoshizawa, S. Miyagi, M. Kawano, K. Ishiguro and M. Fujita, *J. Am. Chem. Soc.*, 2004, **126**, 9172.

9 Y.-R. Zheng, K. Suntharalingam, T. C. Johnstone and S. J. Lippard, *Chem. Sci.*, 2015, **6**, 1189.

10 K. Nakabayashi, M. Kawano, T. Kato, K. Furukawa, S. Ohkoshi, T. Hozumi and M. Fujita, *Chem. – Asian J.*, 2007, **2**, 164.

11 W.-Y. Sun, T. Kusukawa and M. Fujita, *J. Am. Chem. Soc.*, 2002, **124**, 11570.

12 D. Bhattacharya, C. H. Chang, Y. H. Cheng, L. L. Lai, H. Y. Lu, C. Y. Lin and K. L. Lu, *Chem. – Eur. J.*, 2012, **18**, 5275.

13 P. H. Dinolfo, V. Coropceanu, J.-L. Brédas and J. T. Hupp, *J. Am. Chem. Soc.*, 2006, **128**, 12592.

14 P. H. Dinolfo, M. E. Williams, C. L. Stern and J. T. Hupp, *J. Am. Chem. Soc.*, 2004, **126**, 12989.

15 (*a*) F. Würthner, A. Sautter, D. Schmid and P. J. A. Weber, *Chem. – Eur. J.*, 2001, **7**, 894; (*b*) F. Wurthner and A. Sautter, *Chem. Commun.*, 2000, 445.

16 C. C. You and F. Wurthner, *J. Am. Chem. Soc.*, 2003, **125**, 9716.

17 K. Mahata, P. D. Frischmann and F. Wurthner, *J. Am. Chem. Soc.*, 2013, **135**, 15656.

18 (*a*) L. J. Chen, Q. J. Li, J. M. He, H. W. Tan, Z. Abliz and H. B. Yang, *J. Org. Chem.*, 2012, **77**, 1148; (*b*) K. Ghosh, Y. Zhao, H. B. Yang, B. H. Northrop, H. S. White and P. J. Stang, *J. Org. Chem.*, 2008, **73**, 8553; (*c*) H. B. Yang, K. Ghosh, Y. Zhao, B. H. Northrop, M. M. Lyndon, D. C. Muddiman, H. S. White and P. J. Stang, *J. Am. Chem. Soc.*, 2008, **130**, 839.

19 G.-Z. Zhao, Q.-J. Li, L.-J. Chen, H. Tan, C.-H. Wang, D. A. Lehman, D. C. Muddiman and H.-B. Yang, *Organometallics*, 2011, **30**, 3637.

20 K. Ghosh, J. M. Hu, H. B. Yang, B. H. Northrop, H. S. White and P. J. Stang, *J. Org. Chem.*, 2009, **74**, 4828.

21 (*a*) Q. J. Li, G. Z. Zhao, L. J. Chen, H. W. Tan, C. H. Wang, D. X. Wang, D. A. Lehman, D. C. Muddiman and H. B. Yang, *Organometallics*, 2012, **31**, 7241; (*b*) Q. Han, Q. J. Li, J. He, B. Hu, H. Tan, Z. Abliz, C. H. Wang, Y. Yu and H. B. Yang, *J. Org. Chem.*, 2011, **76**, 9660; (*c*) G. Z. Zhao, Q. J. Li, L. J. Chen, H. W. Tan, C. H. Wang, D. X. Wang and H. B. Yang, *Organometallics*, 2011, **30**, 5141; (*d*) G.-Z. Zhao, L.-J. Chen, C.-H. Wang, H.-B. Yang, K. Ghosh, Y.-R. Zheng, M. M. Lyndon, D. C. Muddiman and P. J. Stang, *Organometallics*, 2010, **29**, 6137.

22 K. Ghosh, J. M. Hu, H. S. White and P. J. Stang, *J. Am. Chem. Soc.*, 2009, **131**, 6695.

23 Y. Cohen, L. Avram and L. Frish, *Angew. Chem., Int. Ed.*, 2005, **44**, 520.

24 N. Das, A. M. Arif, P. J. Stang, M. Sieger, B. Sarkar, W. Kaim and J. Fiedler, *Inorg. Chem.*, 2005, **44**, 5798.

25 (*a*) N. Martin, *Chem. Commun.*, 2013, **49**, 7025; (*b*) M. R. Bryce, *J. Mater. Chem.*, 2000, **10**, 589; (*c*) P. Batail, *Chem. Rev.*, 2004, 4887.

26 (*a*) D. Canevet, M. Salle, G. X. Zhang, D. Q. Zhang and D. B. Zhu, *Chem. Commun.*, 2009, 2245; (*b*) J. L. Segura and N. Martin, *Angew. Chem., Int. Ed.*, 2001, **40**, 1372.

27 J. Xiong, W. Liu, Y. Wang, L. Cui, Y.-Z. Li and J.-L. Zuo, *Organometallics*, 2012, **31**, 3938.

28 E. Gontier, N. Bellec, P. Brignou, A. Gohier, M. Guerro, T. Roisnel and D. Lorcy, *Org. Lett.*, 2010, **12**, 2386.

29 (*a*) J. Y. Balandier, M. Chas, P. I. Dron, S. Goeb, D. Canevet, A. Belyasmine, M. Allain and M. Sallé, *J. Org. Chem.*, 2010, **75**, 1589; (*b*) J. Y. Balandier, A. Belyasmine and M. Salle, *Synthesis*, 2006, 2815; (*c*) J. O. Jeppesen and J. Becher, *Eur. J. Org. Chem.*, 2003, 3245; (*d*) J. O. Jeppesen, K. Takimiya, F. Jensen, T. Brimert, K. Nielsen, N. Thorup and J. Becher, *J. Org. Chem.*, 2000, **65**, 5794.

30 (*a*) F. G. Brunetti, J. L. Lopez, C. Atienza and N. Martin, *J. Mater. Chem.*, 2012, **22**, 4188; (*b*) A. J. Moore and M. R. Bryce, *J. Chem. Soc., Perkin Trans. 1*, 1991, 157; (*c*) M. R. Bryce, A. J. Moore, M. Hasan, G. J. Ashwell, A. T. Fraser, W. Clegg, M. B. Hursthouse and A. I. Karaulov, *Angew. Chem., Int. Ed. Engl.*, 1990, **29**, 1450; (*d*) Y. Yamashita, Y. Kobayashi and T. Miyashi, *Angew. Chem., Int. Ed. Engl.*, 1989, **28**, 1052.

31 V. Vajpayee, S. Bivaud, S. Goeb, V. Croué, M. Allain, B. V. Popp, A. Garci, B. Therrien and M. Sallé, *Organometallics*, 2014, **33**, 1651.

32 (*a*) S. B. Nielsen, M. B. Nielsen and H. J. A. Jensen, *Phys. Chem. Chem. Phys.*, 2003, **5**, 1376; (*b*) R. Andreu, J. Garin and J. Orduna, *Tetrahedron*, 2001, **57**, 7883.

33 J. Lau, P. Blanchard, A. Riou, M. Jubault, M. P. Cava and J. Becher, *J. Org. Chem.*, 1997, **62**, 4936.

34 (*a*) T. K. Hansen, T. Jorgensen, F. Jensen, P. H. Thygesen, K. Christiansen, M. B. Hursthouse, M. E. Harman, M. A. Malik, B. Girmay, A. E. Underhill, M. Begtrup, J. D. Kilburn, K. Belmore, P. Roepstorff and J. Becher, *J. Org. Chem.*, 1993, **58**, 1359;

(*b*) T. Jorgensen, J. Becher, T. K. Hansen, K. Christiansen, P. Roepstorff, S. Larsen and A. Nygaard, *Adv. Mater.*, 1991, **3**, 486.
35 S. Goeb, S. Bivaud, V. Croué, V. Vajpayee, M. Allain and M. Sallé, *Materials*, 2014, **7**, 611.
36 J.-Y. Balandier, M. Chas, S. Goeb, P. I. Dron, D. Rondeau, A. Belyasmine, N. Gallego and M. Sallé, *New J. Chem.*, 2011, **35**, 165.
37 S. Goeb, S. Bivaud, P. I. Dron, J.-Y. Balandier, M. Chas and M. Sallé, *Chem. Commun.*, 2012, **48**, 3106.
38 (*a*) D. Canevet, E. M. Pérez and N. Martín, *Angew. Chem., Int. Ed.*, 2011, **50**, 9248; (*b*) E. M. Perez and N. Martin, *Chem. Soc. Rev.*, 2008, **37**, 1512.
39 (*a*) S. Bivaud, S. Goeb, J. Y. Balandier, M. Chas, M. Allain and M. Salle, *Eur. J. Inorg. Chem.*, 2014, 2440; (*b*) S. Bivaud, J. Y. Balandier, M. Chas, M. Allain, S. Goeb and M. Sallé, *J. Am. Chem. Soc.*, 2012, **134**, 11968.
40 S. Bivaud, S. Goeb, V. Croue, P. I. Dron, M. Allain and M. Sallé, *J. Am. Chem. Soc.*, 2013, **135**, 10018.
41 (*a*) B. Therrien, *Nanomaterials in Drug Delivery, Imaging, and Tissue Engineering*, John Wiley & Sons, Inc., 2013, p. 145; (*b*) T. R. Cook, V. Vajpayee, M. H. Lee, P. J. Stang and K. W. Chi, *Acc. Chem. Res.*, 2013, **46**, 2464; (*c*) B. Therrien, in *Chemistry of Nanocontainers*, ed. M. Albrecht and E. Hahn, Springer, Berlin, Heidelberg, 2012, vol. 319, p. 35.
42 J. Mattsson, P. Govindaswamy, A. K. Renfrew, P. J. Dyson, P. Štěpnička, G. Süss-Fink and B. Therrien, *Organometallics*, 2009, **28**, 4350.
43 S. Shanmugaraju, D. Samanta and P. S. Mukherjee, *Beilstein J. Org. Chem.*, 2012, **8**, 313.
44 D. Samanta, S. Shanmugaraju, A. A. Adeyemo and P. S. Mukherjee, *J. Organomet. Chem.*, 2014, **751**, 703.
45 V. Vajpayee, Y. H. Song, Y. J. Yang, S. C. Kang, T. R. Cook, D. W. Kim, M. S. Lah, I. S. Kim, M. Wang, P. J. Stang and K. W. Chi, *Organometallics*, 2011, **30**, 6482.
46 Y.-F. Han, Y.-J. Lin, W.-G. Jia and G.-X. Jin, *Organometallics*, 2008, **27**, 4088.
47 (*a*) J. E. M. Lewis, A. B. S. Elliott, C. J. McAdam, K. C. Gordon and J. D. Crowley, *Chem. Sci.*, 2014, **5**, 1833; (*b*) J. E. M. Lewis, C. John McAdam, M. G. Gardiner and J. D. Crowley, *Chem. Commun.*, 2013, **49**, 3398.
48 F. Jiang, N. Wang, Z. Du, J. Wang, Z. Lan and R. Yang, *Chem. – Asian J.*, 2012, **7**, 2230.
49 S. S. Sun and A. J. Lees, *Inorg. Chem.*, 2001, **40**, 3154.
50 L. A. Berben, M. C. Faia, N. R. Crawford and J. R. Long, *Inorg. Chem.*, 2006, **45**, 6378.
51 (*a*) N. Shan, J. D. Ingram, T. L. Easun, S. J. Vickers, H. Adams, M. D. Ward and J. A. Thomas, *Dalton Trans.*, 2006, 2900; (*b*) N. Shan, S. J. Vickers, H. Adams, M. D. Ward and J. A. Thomas, *Angew. Chem., Int. Ed.*, 2004, **43**, 3938.
52 M. Frank, J. Hey, I. Balcioglu, Y.-S. Chen, D. Stalke, T. Suenobu, S. Fukuzumi, H. Frauendorf and G. H. Clever, *Angew. Chem., Int. Ed.*, 2013, **52**, 10102.
53 M. Frank, L. Krause, R. Herbst-Irmer, D. Stalke and G. H. Clever, *Dalton Trans.*, 2014, **43**, 4587.
54 P.-C. Lin, H.-Y. Chen, P.-Y. Chen, M.-H. Chiang, M. Y. Chiang, T.-S. Kuo and S. C. N. Hsu, *Inorg. Chem.*, 2011, **50**, 10825.
55 M. Lahav, R. Gabai, A. N. Shipway and I. Willner, *Chem. Commun.*, 1999, 1937.
56 (*a*) J. E. M. Lewis, E. L. Gavey, S. A. Cameron and J. D. Crowley, *Chem. Sci.*, 2012, **3**, 778; (*b*) I. A. Riddell, M. M. J. Smulders, J. K. Clegg and J. R. Nitschke, *Chem. Commun.*, 2011, **47**, 457; (*c*) P. Mal, D. Schultz, K. Beyeh, K. Rissanen and J. R. Nitschke, *Angew. Chem., Int. Ed.*, 2008, **47**, 8297; (*d*) F. Ibukuro, T. Kusukawa and M. Fujita, *J. Am. Chem. Soc.*, 1998, **120**, 8561.
57 J. L. Boyer, M. Ramesh, H. Yao, T. B. Rauchfuss and S. R. Wilson, *J. Am. Chem. Soc.*, 2007, **129**, 1931.